IJASRM
International Journal of Advanced Scientific Research and Management, Volume 4 Issue 5, May 2019
www.ijasrm.com
ISSN 2455-6378

Dynamic Mechanical Properties of a Newly Developed Bio-based Eco-Friendly Polyurethane (PU) Coating for Outer Structure Applications in Aeronautical Industries

Abhishek CHANDRAMOHAN[1] and Prashaant CHANDRAMOHAN[1]

[1] VPA Laboratory Private Limited, Chennai, Tamil Nadu, 600045, India

Abstract

The development of protective coatings in aeronautical industries have encouraged many possibilities and one such is organic coatings. For long, chemical industries have been demanding eco-friendly polymers to replace non-biodegradable materials. Although paints provides good resistance to corrosion, organic coatings can be tailored made to improve additional properties such as electrical conductivity, resistance to ultra-violet radiations, viscoelastic properties and etc. In this work, a bio-based polymer i.e., non-isocyanate polyurethane (NIPU) is synthesized by introducing fine boron carbide (B_4C) powder at later stages of preparation. B_4C is known for its extreme hardness, which results in a super coating when introduced in thin films. The goal is to replace paints with thin films to be more eco-friendly to the environment. The coating is synthesized in such a way that the presence of B_4C provides better resistance against damages due to rupture mechanisms. Hence, dynamic mechanical analysis of the newly developed polymer were performed to understand its viscous behaviours.

Keywords – Constant strain rate, Creep, Dynamic mechanical analysis, Nanoindentation, Polymer coating, Strain rate sensitivity.

1. Introduction

Since the 1970s, fibre reinforced composites have been used in the aeronautical sector for applications requiring better stiffness, as well as resistance to weight ratio. The thermoset resins can be used for protecting metal substrates when applied as a coating. Epoxy is a family of thermoset resins that are widely used for coating purposes. However, the properties of these polymers have proved insufficient to meet the stringent requirements (use of non-toxic degradable materials) that are necessary in the field of aviation concerning the environment. Therefore, new solutions for high performance coatings i.e. better resistance to corrosion, rupture and etc., while avoiding the use of chromates and toxic compounds during preparation are deemed necessary.

The synthesis of organic polymers, whose properties are more efficient than those of epoxies have many potential applications. The chemical industries favour bio-based protective coatings due to their short gel time and resistance to corrosion in order to replace the non-renewable raw materials. Hence, this work focuses on producing a compound that is bio-based, which also provides better resistance against rupture mechanisms.

PUs are extremely popular in applications such as coatings and adhesives because of its physio-chemical properties. This in turn provides better mechanical properties by interacting well within the matrix. However, one of the compounds used in the synthesis of PU is produced from phosgene i.e., isocyanate, which is a highly toxic compound. Recent developments in synthesis of NIPUs have contributed in creating different functional groups through various compounds. NIPUs has better stability in their hydroxyl groups, which signifies that it is better than conventional PUs in terms of degradation [1], [2].

IJASRM
International Journal of Advanced Scientific Research and Management, Volume 4 Issue 5, May 2019
www.ijasrm.com
ISSN 2455-6378

2. Synthesis of Composite

The specimen were prepared in three stages: anodization, polymer coating and additive integration. The multilayers (Fig. 1) consists of an unclad Al 2024-T3 of 4 mm thickness that is anodized up to 3 µm thickness. The anodization setup used was similar to the techniques by Alexis RENAUD et al. [3]. The Al plate was placed at the anode in a sulfo-tartaric acid electrolytic bath (40g/L H2SO4 + 80g/L C4H6O6) at 40°C and 10 V for 25 min. The anodization process creates a rough layer with structured porosity perpendicular to the surface. The resulting oxide layer accommodates the polymer coating mechanically by promoting strong adhesion with better surface interactions. The anodic layer was then bar-coated with NIPU for 100 µm thickness. NIPU was synthesized similar to the method demonstrated by Mariusz Tryznowski et al. [4]. By polyaddition of poly(cyclic carbonate)s, bis(cyclic carbonate) 2 was synthesized. It was then used as monomer with diamines through green route for the preparation of NIPU. The obtained NIPU is bio-based and environmental friendly with glass transition temperature (T_G) of 40°C. The low T_G signifies high thermal stability. Immediately after the coating of NIPU over the anodic layer, fine B_4C powder of 99% were dusted on top. The aim of the polymer coating is to replace the paints in aeronautical industries for a more eco-friendly environment. Similarly, the use of B_4C powder is to provide better resistance against rupture mechanisms as they are known for extreme hardness. The multilayers are then cured at room temperature.

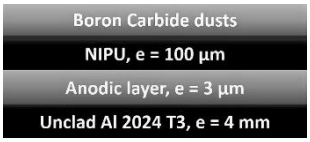

Fig. 1. Schematic of multilayers

3. Experiment

Viscoplasticity attributes both viscous and plastic properties of the material. The plasticity is defined by the inelastic properties i.e. unrecoverable deformation when a load is applied, which is time-dependent. Such behaviours can be studied under strain rate sensitivity (SRS) methods in nanoindentation. Through power law, the strain rate defines the plastic stresses that can be sustained in a material, where higher strain rates signifies higher plastic stresses. In other words, the strain rate signifies both shrinkage and expansion of the material. The expression is given as [5]:

$$m = \frac{\partial \ln \sigma}{\partial \ln \varepsilon^p}\Big|_{\varepsilon,T} \geq 0 \quad (1)$$

Where m = SRS coefficient, σ = stress, ε = strain, ε^p = plastic strain and T = temperature.

In case of thin films, there exists influence of the substrate. The phenomenon accounts for overestimation of hardness (H) since apparent hardness of thin films changes when the indenter senses the underlying substrate. When it is assumed that SRS does not exist on the substrate, the relationship is given by [5]:

$$m_{apparent} = \frac{\partial \ln H_{measured}}{\partial \ln \dot{e}} \quad (2)$$

$$H_{measured} = \hat{H}(H_f, H_s, h) \quad (3)$$

Where ė = strain rate, $\hat{H}(H_f, H_s, h)$ = apparent hardness as a function of hardness of the film and substrate and, h = depth.

In constant load and hold test (CLH) or creep test, the load 'P' is held constant over certain period by setting a limit, where the indentation depth is recorded as f(t) i.e. load-controlled mode. Creep occurs when the material is long exposed to high stress levels below the yield point. Therefore, creep tests are useful in studying delayed deformation of polymers under mechanical stresses, which signifies that the recovery is proportional to the stress applied at given time. ė is determined from [6]:

$$\dot{e} = \frac{d \ln S}{dt} \quad (4)$$

Where S = stiffness.

In constant strain rate test (CSR), the specimen is loaded at constant load strain rate ($\dot{e}_P$) since the indenter is load controlled. This method relies on the assumption that the hardness does not vary with depths for a geometrically self-similar indenter i.e. conical or pyramid. ė is determined from [6]:

$$\dot{e}_P = \frac{d \ln h}{dt} \quad (5)$$

The tests shares the principles of continuous stiffness measurement (CSM) in nanoindentation (Fig. 2. A), where the loading is performed at a constant load rate. The underlying principle involves applying oscillations to overall loading, where unloading is eliminated (Fig. 2. B). This in turn

IJASRM
International Journal of Advanced Scientific Research and Management, Volume 4 Issue 5, May 2019
www.ijasrm.com
ISSN 2455-6378

creates an in-phase and out-of-phase components from load-displacement response, which provides accurate results by identifying the initial surface contact between the indenter and the specimen. The CSM oscillation is maintained during the holding period and hence, the indentation depth is directly calculated by using contact stiffness to avoid thermal drifts.

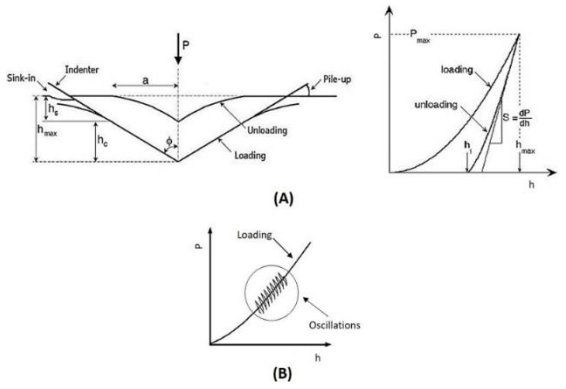

Fig. 2. (A). Instrumented nanoindentation mechanism with corresponding 'h vs P' curve and, (B). Principle of CSM

4. Results and Discussions

4.1. Creep test (CLH) – SRS

With maximum load (P_{max}) of 10 mN, loading time of 1.6 s and holding segment of 600 s, the time series becomes $t_n = t_{n-1} + 0.33$ s (experiment setting) in load-time plots (Fig. 3). From Fig. 4, it is shown that the total creep time lies within 1700 nm and 6400 nm depth range and the recovery time lies within 6400 nm and 6200 nm depth range. The recovery time period is directly proportional to T_G, which in turn depends on the curing of polymers. From a thermomechanical point of view, low T_G (40°C) signifies less internal stress accumulation in the material. Under maximum load-holding (Fig. 4), the recovery time is less than creep time and hence, the recovery at unloading is not equal to creep deformation [7]. If both are equal then it signifies the failure of structural integrity of the polymer.

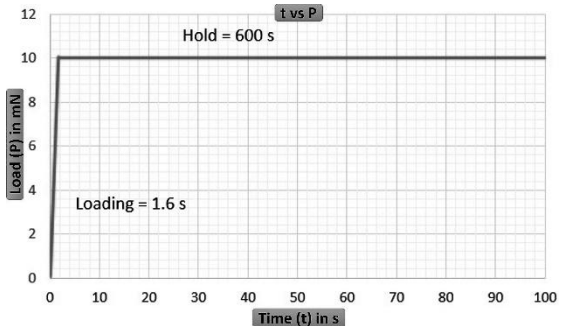

Fig. 3. t vs P

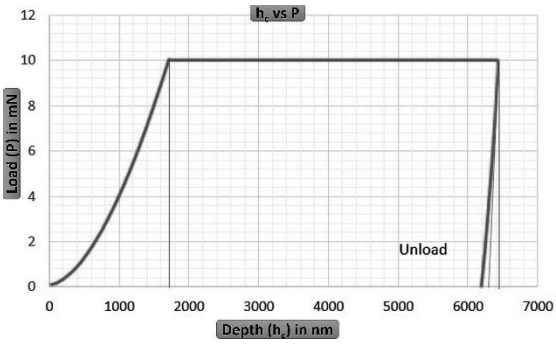

Fig. 4. h_c vs P

h_c (Fig. 5) increases rapidly for first 100 s, where a total of 44.1% increase was observed for 600 s. At the same time period, S (Fig. 5) increases only by 20%. Theoretically, the difference signifies the effect of pile-up and sink-in parameters ($c = \frac{h_c}{h}$) as illustrated in Fig. 2. A. If S% > h_c% then c decreases with t. The decrease in c signifies that the material creeps with small stress exponent [8]. From Fig. 6, it is observed that creep modulus (E) decreases with increasing h_c and the value over the range were measured as 1.8 GPa. This modulus is theoretically proportional to load / area (P / A) ratio.

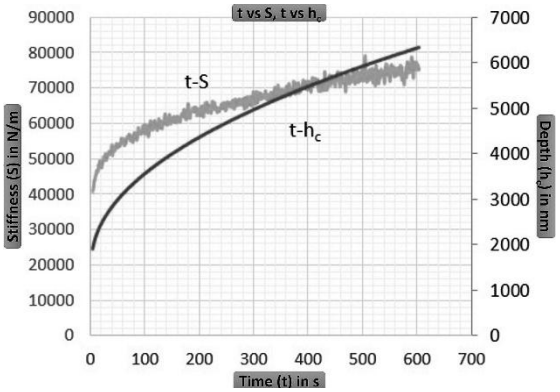

Fig. 5. t vs S, t vs h_c

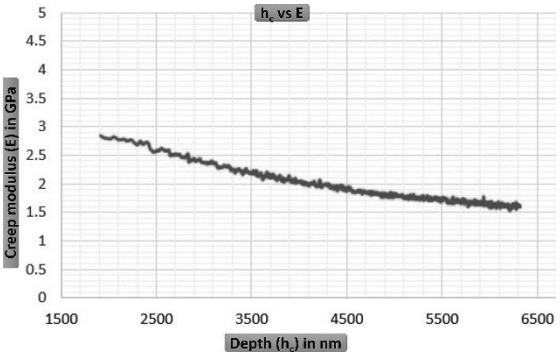

Fig. 6. h_c vs E

IJASRM
International Journal of Advanced Scientific Research and Management, Volume 4 Issue 5, May 2019
www.ijasrm.com
ISSN 2455-6378

From Fig. 7, the first 100 s of the time segment in 't vs ė' is represented by primary creep. Whereas, it is steady for the next 300 s covering the secondary creep. The mean stress (σ_{mean} = H = P / A) for the same time segment (Fig. 7) resulted in an 80% decrease from the initial point. This is because when t is increased, h_c increases and σ_{mean} decreases (σ_{mean} = 0.02 GPa over the range), σ_{mean} decreases because A increases along with h_c, where A is inversely proportional to σ_{mean} i.e., $[t \propto h_c \propto A] \propto \frac{1}{\sigma_{mean}}$. Therefore, the steady decrease in ė and σ_{mean} confirms the time-dependent deformation of the material [9].

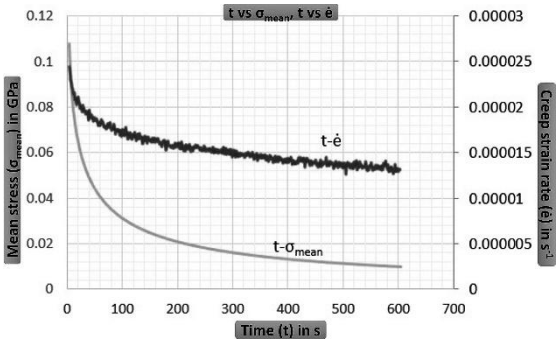

Fig. 7. t vs σ_{mean}, t vs ė

4.2. CSR – SRS

In addition to overcoming thermal drifts (similar to CLH) and different target strain rates, the difference in determining m from CSR over CSM is that the depth corrections can be avoided which are based on apparent depth [6]. The tests were performed at different $\dot{e}_P$ of 0.005 s^{-1}, 0.025 s^{-1} and 0.1 s^{-1}. Fig. 8. shows continuous modulus for different $\dot{e}_P$, where the moduli decreases with indentation time i.e. $t_n = t_{n-1}$ + 0.05 s (experiment setting). The moduli continues to decrease steadily, where $E_{0.005}$ over the range were measured as 4.4 GPa and both $E_{0.025}$, $E_{0.1}$ as 3.8 GPa.

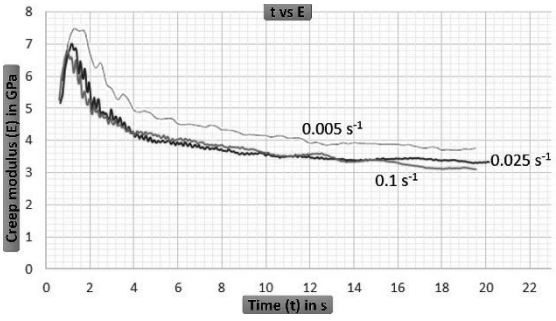

Fig. 8. t vs E for different $\dot{e}_P$

Fig. 9. plots the mean stress as a function of strain rate i.e., $\ln H \; vs \frac{d \ln h}{dt}$, where the logarithmic scale is equivalent to the power law relationship from a uniaxial test. For $\dot{e}_P$ of 0.005 s^{-1}, 0.025 s^{-1} and 0.1 s^{-1}, the values of m were measured as 15.3, 14.7 and 18 respectively. As seen from Fig. 9, steady states were achieved for different conditions of $\dot{e}_P$. Since $\dot{e}_P$ is kept constant in CSR, the volume of expansion of the material is controlled i.e. softening and hardening [10]. Therefore, the deformation is directly proportional to $\dot{e}_P$ in CSR.

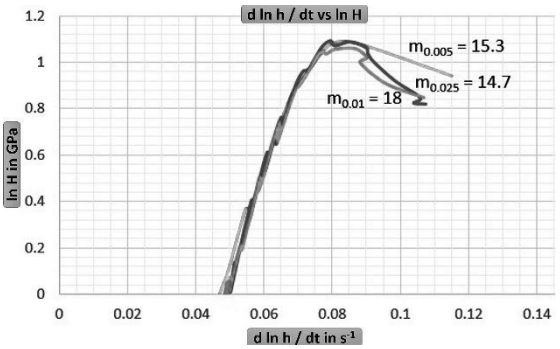

Fig. 9. ė vs σ_{mean} for different $\dot{e}_P$

5. Conclusion

A new composite was synthesized in this work to find its application as a replacement product for paints in aeronautical industries. The mechanical properties of the bio-based eco-friendly coating were determined from nano-experiments under dynamic conditions. By the principle of CSM, a steady state and controlled deformations were observed in CSR. The highlight of the research is the introduction of B_4C powder in the polymer layer, where the goal was also to provide better resistance against rupture mechanisms. It is to be noted that any specific properties can be improved ex: resistance to impact, UV radiation, corrosion and etc. by changing the formulations in the functional group of polymers.

References

[1] Delebecq E, Pascault J.P, Boutevin B, Ganachaud F, On the versatility of urethane/urea bonds : Reversibility, blocked isocyanate, and non-isocyanate polyurethane. Chemical Reviews, 113(1): 80-118, (2012).
[2] Chattopadhyay D.K, Raju K.V.S.N, Structural engineering of polyurethane coatings for high performance applications. Progress in Polymer Science, 32(3): 352-418, (2007).
[3] Renaud A, Poorteman M, Escobar J, Dumas L, Paint Y, Bonnaud L, Dubois P, Olivier M.G, A new corrosion protection approach

for aeronautical applications combining a Phenol-paraPhenyleneDiAmine benzoxazine resin applied on sulfo-tartaric anodized aluminium. Progress in Organic Coating, 112: 278-287, (2017).

[4] Tryznowski M, Swiderska A, Zołek-Tryznowska Z, Gołofit T, Parzuchowski P.G, Facile route to multigram synthesis of environmentally friendly non-isocyanate polyurethanes, Polymer, 80: 228-236, (2015).

[5] Maier-Kiener V, Durst K, Advanced nanoindentation testing for studying strain-rate sensitivity and activation volume, Journal of the Minerals, Metals & Materials Society, 69(11): 2246-2255, (2017).

[6] Su C, Herbert E.G, Sohn S, LaManna, J.A, Oliver W.C, Pharr G.M, Measurement of power-law creep parameters by instrumented indentation methods, Journal of the Mechanics and Physics of Solids, 61(2): 517-536, (2013).

[7] Yang S, Zhang Y.W, Zeng K, Analysis of nanoindentation creep for polymeric materials, Journal of Applied Physics, 95(7): 3655-3666, (2004).

[8] Rar A, Sohn S, Oliver W.C, Goldsby D.L, Tullis T.E, Pharr G.M, On the measurement of creep by nanoindentation with continuous stiffness techniques, Materials Research Society, 841: R4.2.1-R4.2.6, (2005).

[9] Bhushan B, Li X, A review of nanoindentation continuous stiffness measurement technique and its applications, Materials Characterization, 48(1): 11-36, (2002).

[10] Alkorta J, Martínez-Esnaola J.M, Sevillano J.G, Critical examination of strain-rate sensitivity measurement by nanoindentation methods: Application to severely deformed niobium, Acta Materialia, 56(4): 884-893, (2008).